

Representation of the conic departure from a sphere over an off-axis aperture

Robert E. Parks
Optical Perspectives Group

Background: It is often useful to understand the topography or 3-dimensional shape of a conic surface from its nearest spherical surface over an off-axis aperture. For example, if one wants to determine the difficulty of fabricating an off-axis conical mirror as a stand alone element rather than coring it out of a symmetric parent mirror, understanding the shape of this off-axis surface is necessary. This same understanding is useful for calculating the maximum size lap that will fit an aspheric mirror within a certain tolerance.

In this paper we frame the problem from the view point of testing a conic mirror at its center of curvature and ask what does the departure from a spherical shape look like over an off-axis aperture. The analysis is done using Zernike polynomials through third order. While their use is not necessary and their formalism somewhat obscures the process at first, this same formalism affords great insight to many optical testing situations once a familiarity with these polynomials is gained.

Departure of a symmetric conic mirror from its vertex sphere: We begin with the exact representation of the sag of a symmetric conic mirror, namely

$$z = \frac{c_v r^2}{1 + \left[1 - (\kappa + 1)c_v^2 r^2\right]^{1/2}} \quad (1)$$

Here the origin of coordinates is at the vertex of the conic mirror, r is the radial coordinate in the aperture, $c_v = 1/R_v$ is the vertex curvature and κ is the conic constant of the mirror ($\kappa = 0$ for a sphere and $\kappa = -1$ for a parabola). If Eq. (1) is expanded in a power series we have

$$z = \frac{c_v r^2}{2} + \frac{(\kappa + 1)c_v^3 r^4}{8} + \dots \quad (2)$$

By using this same expansion for the case of a sphere where $\kappa = 0$ and subtracting it from Eq. (2) for the conic we get the departure of the conic from its vertex sphere to third order as shown in Figure 1 and in Eq. (3).

$$\delta z = \frac{\kappa c_v^3 r^4}{8} + \dots \quad (3)$$

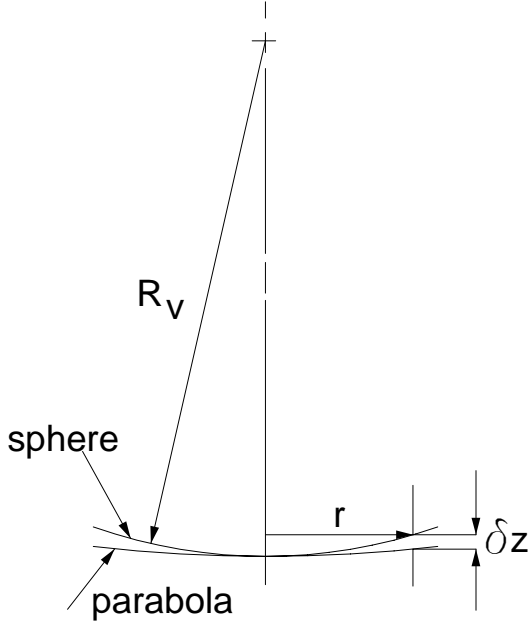


Fig. 1

Departure of conic from vertex sphere

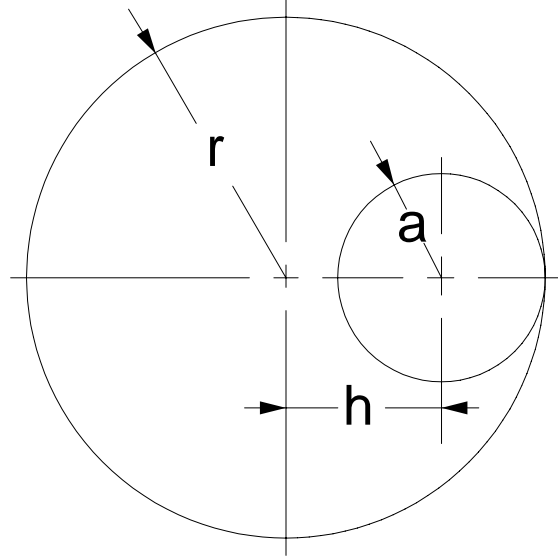


Fig. 2

Geometry of off-axis aperture

Departure of an off-axis conic mirror from its best fit sphere: Consider the off-axis aperture in Fig. 2 centered a distance h off-axis with a pupil radius of a . While Eq. (3) is valid over all of the symmetric mirror, our interest is only in the departure over the off-axis aperture. In many cases this is the only place there will be any glass to test. To find the behavior of δz over the off-axis aperture the origin of coordinates must be shifted by h so that

$$x = x' + h \text{ and } y = y' \quad (4)$$

where the primed coordinates are centered about the vertex of the off-axis aperture. At the same time the analysis must be performed over a normalized aperture since this is the only place where the Zernike polynomials are defined. To do this, let

$$x' = ax'' \text{ and } y' = ay'' \text{ so that } x''^2 + y''^2 = \rho^2 \text{ where } 0 \leq \rho \leq 1. \quad (5)$$

When the transformed variables are substituted in Eq. (3) we have

$$\delta z = \frac{\kappa c_v^3}{8} \left[(ax'' + h)^2 + (ay'')^2 \right]^2 \quad (6)$$

Upon expanding this expression and equating like powers of x'' and y'' with those of the low order Zernike polynomials we find the coefficients of the polynomial terms to be

$$\begin{aligned}
 b_4^0 &= \frac{\kappa c_v^3 a^4}{48} \text{ (spherical aberration)} & b_3^1 &= \frac{\kappa c_v^3 a^3 h}{6} \text{ (coma)} \\
 b_2^2 &= \frac{\kappa c_v^3 a^2 h^2}{4} \text{ (astigmatism)} & b_2^0 &= \frac{\kappa c_v^3 (4a^2 h^2 + a^4)}{16} \text{ (focus)} \quad (7) \\
 b_1^1 &= \frac{\kappa c_v^3 (3ah^3 + 2a^3 h)}{3} \text{ (tilt)} & b_0^0 &= \frac{\kappa c_v^3 (3h^4 + 6a^2 h^2 + a^4)}{24} \text{ (piston)}
 \end{aligned}$$

Using these coefficients the sag over the off-axis aperture is expressed as

$$\delta z = b_4^0 U_4^0 + b_3^1 U_3^1 + b_2^2 U_2^2 + b_2^0 U_2^0 + b_1^1 U_1^1 + b_0^0 U_0^0, \quad (8)$$

where the $U_n^{\pm m}(\rho, \theta)$ are the corresponding Zernike polynomial terms. Eq. (8) can best be understood by considering it as a linear combination of six basis surfaces representing third order spherical aberration, coma, astigmatism, power, tilt and piston. In the left hand part Figure 3a we show the symmetrical parent mirror while in Figure 3b we show the off-axis aperture now expanded to the unit circle.

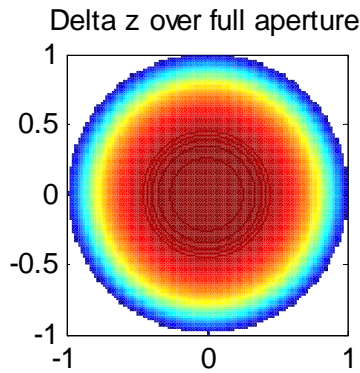


Fig. 3a

$a_{0,0} = -8.000$
 $a_{-1,1} = 0.000$
 $a_{1,1} = 0.000$
 $a_{-2,2} = 0.000$
 $a_{0,2} = -12.00$
 $a_{2,2} = 0.000$
 $a_{-3,3} = 0.000$
 $a_{-1,3} = 0.000$
 $a_{1,3} = 0.000$
 $a_{3,3} = 0.000$

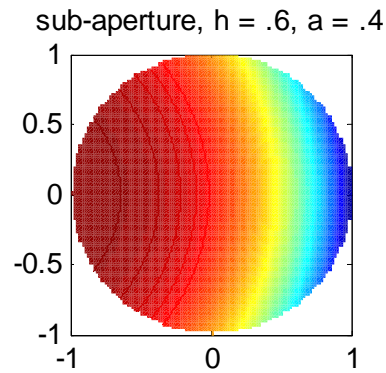


Fig. 3b

$a_{0,0} = -2.026$
 $a_{-1,1} = 0.000$
 $a_{1,1} = -3.583$
 $a_{-2,2} = 0.000$
 $a_{0,2} = -1.024$
 $a_{2,2} = -0.921$
 $a_{-3,3} = 0.000$
 $a_{-1,3} = 0.000$
 $a_{1,3} = -0.410$
 $a_{3,3} = 0.000$

In Fig. 3a we have δz as given in Eq. 3 while in Fig 3b we have the topography over the off-axis aperture of radius .4 and off-axis distance $h = .6$. The map coloring makes it look like both contours have the same peak-to-valley height but that is

because we have left the auto-scaling for the plots on. In Fig. 5 auto-scaling is turned off so the magnitude of the different basis surfaces becomes clearer.

Clearly Fig. 3b has the character and orientation one would expect of a subaperture six-tenths of the way out the x axis. But it is also clear that if one were doing interferometry to test the surface one would either tilt the reference flat in the interferometer or shift the interferometer laterally to remove the tilt. This same thing can be accomplished by setting the tilt coefficient to 0. The piston coefficient will likewise be set to 0 because the auto-scaling already removes the effect of tilt. The contour map in Fig. 4a shows the shape of the off-axis aperture with piston and tilt removed.

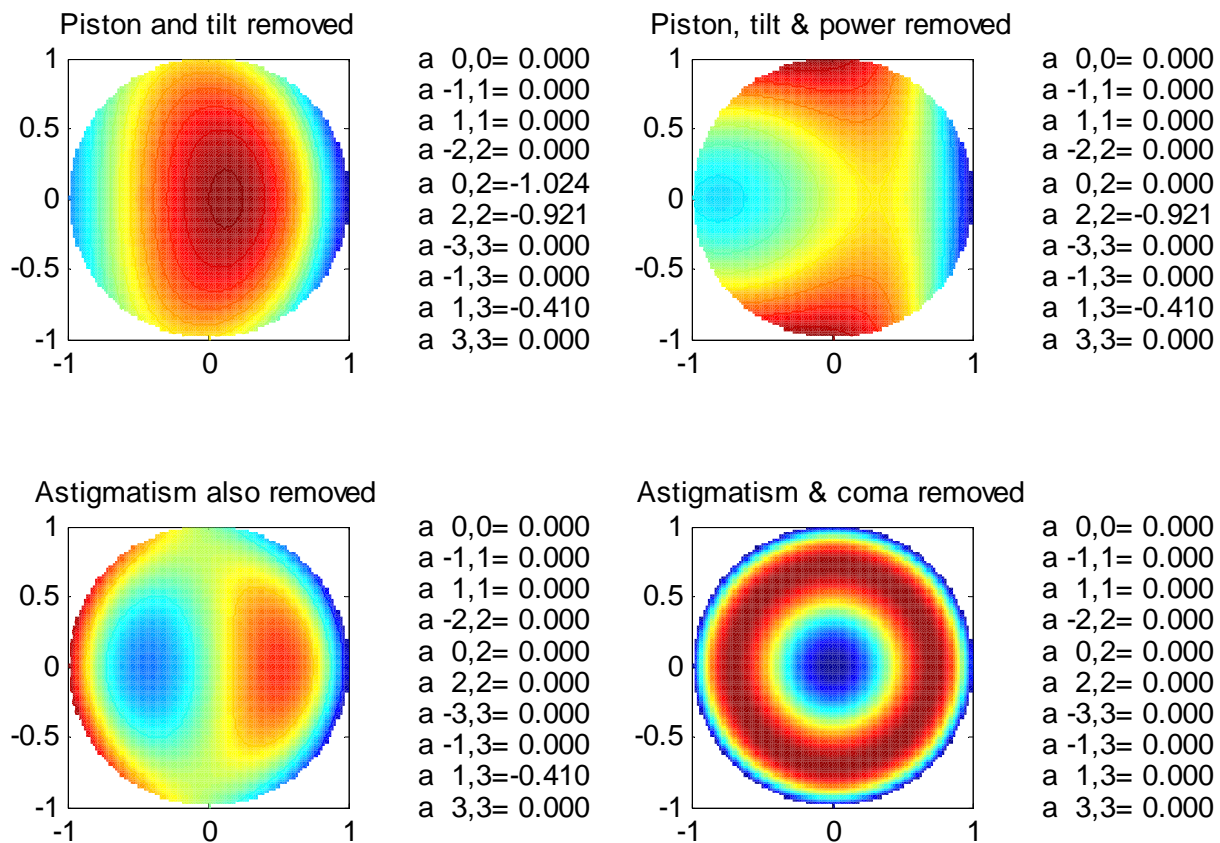


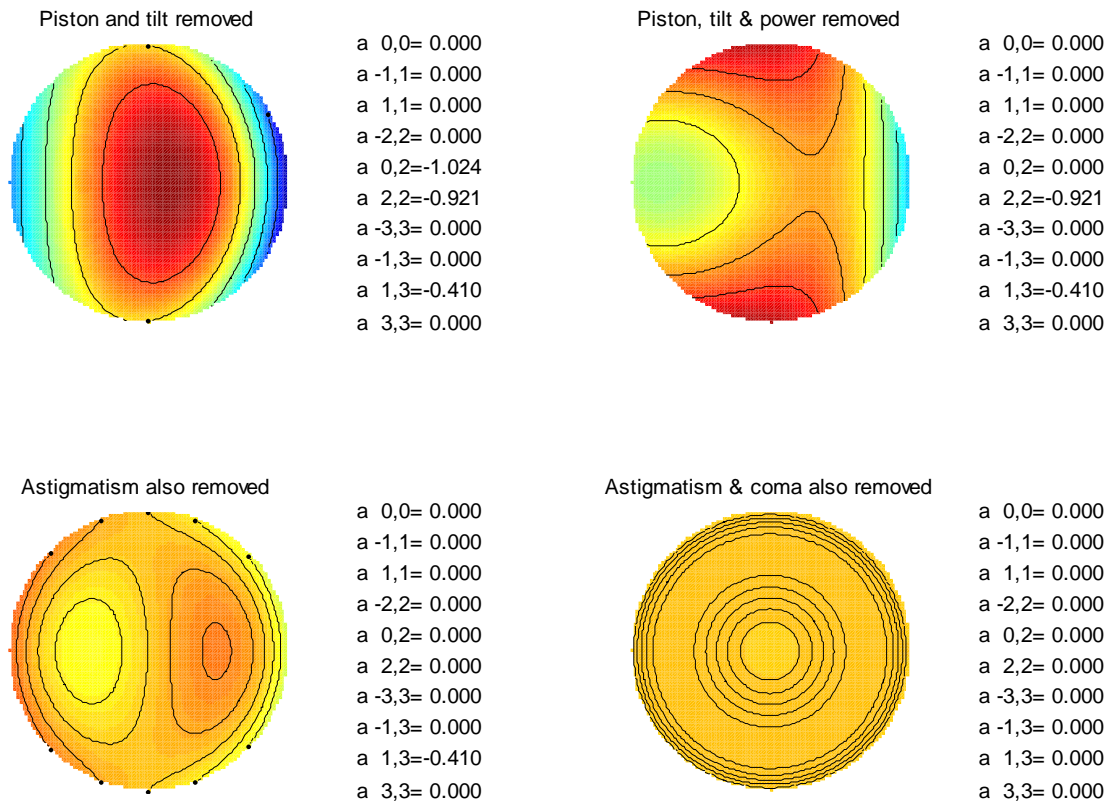
Fig. 4 Residual errors left in the off-axis aperture after removing, upper left, piston and tilt, upper right, piston, tilt and power, lower left, piston, tilt, power and astigmatism, and lower right, piston, tilt, power, astigmatism and coma.

Since the first 10 Zernike coefficients for each contour map are printed beside the map it is easy to see that the piston and tilt have been set to 0. Now the map contains convex power because the radius of curvature of the off-axis aperture is

longer than the vertex radius of the full aperture. Again, if interferometry was being done the interferometer would be backed away from the mirror under test to remove as much focus or power as possible by correcting the alignment. Then the figure would look like that in Fig. 4b.

The astigmatism and other higher order aberrations cannot be removed by any further alignment. These are part of the mirror figure over the off-axis aperture. However, this does show that the major source of error is astigmatism and if there is an easy way to introduce this into the part then one is a long ways toward making an off-axis conic. Fig. 4c shows the topography after the astigmatism is removed and finally, Fig. 4d shows the mirror with the coma removed. This final figure shows there is still some rotationally symmetric error in the part, but very little as is obvious from Fig. 5.

In Fig. 5 we auto-scaling has been turned off and the residual error is plotted relative to the peak-to-valley error after the tilt has been removed. As is clear, a major portion of the error can be removed by just realigning the test set up. It is also clear that one can easily estimate the difficulty of making an off-axis conic mirror or to decide whether a toroidal mirror would be an adequate substitute for an off-axis mirror in some circumstances.



In Fig. 5 above, we have used the same limits on the color scale on all 4 parts of the figure so that it is clear the peak to valley error is less as the aberrations are removed. However, we have added contour lines to illustrate that the shape of the residual errors is the same as in Fig. 4. Figs. 4 and 5 can be compared to get a feel for how much the peak to valley decreases as each aberration is removed.

Conclusion: With this example we have shown several things about the topography of an off-axis portion of a symmetric conic mirror. First, the off-axis topography is made up of a linear combination (or addition) of basis surfaces. These basis surfaces consist of all orders of surfaces up to and including a surface of the same order as that in the original symmetric surface. These basis surfaces are a function of the magnitude of the topography of the symmetric surface, the relative size of the sub-aperture and the position of the sub-aperture within the symmetric aperture. Finally, that a significant amount of the apparent residual error can be removed by simply realigning the test device to the subaperture.